Successes and failures of the live-attenuated influenza vaccine, can we do better?

Laura Matrajt[a], M. Elizabeth Halloran[a,b], Rustom Antia[c]

March 12, 2019

[a]Vaccine and Infectious Disease Division, Fred Hutchinson Cancer Research Center, Seattle, WA 98109
[b]Department of Biostatistics, University of Washington, Seattle, WA 98195
[c]Emory University, Atlanta, GA 30322

Supplemental Material (SM)

Antigenic distance

We are interested in quantifying how negative interference affects the effectiveness of the LAIV, as a function of three antigenic distances: the distances between the vaccine strain, pre-existing immunity, and the challenge strain. For our simulations, we chose the antigenic distance defined by Smith *et al* in [1]. In their paper, Smith *et al* assumed that receptors in B-cells, antibodies and viruses could be represented as a string with 20 symbols, and each symbol could take 4 possible values. They defined the distance between two of those strings utilizing the "Hamming distance" defined to be the number of changes, or *point mutations* needed to go from one string representing one antigen to another [1]. Here, we utilize that antigenic distance and transform it into a match percentage where $d = 0\%$ is a perfect match, while $d = 100\%$ implies that the antibody receptors and the virus are totally different. For example, a Hamming distance of 5 between an antibody and a virus means that we need 5 changes to go from the string representing the antibody to the string representing the virus. Equivalently, we know that $5/20$ receptors are different, or that the antibody and the virus are 25% different. Analogously to Skowronski *et al* [2], who utilized the same antigenic distance, we assume that once the antigenic distance is 4 (or equivalently, $4/20$ receptors are different, or 20% different), the antibodies are no longer cross-reactive.

We now incorporate this antigenic distance into our mathematical models. In order to do this, we utilize a Hill function given by

$$f(d) = \frac{-Md^p}{K^p + d^p} + 1$$

where M, K, and p are parameters to be determined, and d is the antigenic distance between a virus and a B-cell or antibody clone. This function will take the antigenic distance defined above, given as a match percentage through the variable d, and will return an affinity $f(d)$. We use this affinitfy $f(d)$ in our differential equations to modulate the extent to which, antibodies from different clones, will bind (and consequently neutralize), a virus at a given antigenic distance. We also use this affinity function $f(d)$ to modulate the B-cell clone expansion. For our simulations, we chose the following parameters: $M = -1, K = 10$ and $p = 15$, the resulting function $f(d)$ can be seen in figure S1.

We note that here we used the antigenic distance given in [1], but any antigenic distance based on antibody-virus binding properties is suitable, such as distances based on HI assays (*e.g* [1, 3, 4]) or the *p-epitope* distance [5] provided that it can be transformed into a match percentage.

Mathematical models

In this section we present four models of increasing complexity considered in the present work. For each model, we divide the B-cell population into n discrete clones, with different clones having different affinities to different viruses. Conceptually, the effectiveness of antibody-binding and the stimulation of B-cells depend on the antigenic distance between the virus and the B-cells.

The models are based on earlier models [6–10], and described in more detail below.

Model 1: The simplest possible model of interactions between influenza viruses and the immune system consist of a model involving virus V and B-cells. B-cells proliferate at a rate σ depending on the concentration of virus. The B-cell population is divided into n distinct clones, where each clone B_i ($i = 1, \ldots, n$) has a different efficacy to eliminate virus depending on their antigenic distance d_i to it. For each clone, the function $f(d_i)$ described above modulates the ability of that clone to control the virus, as a function of the distance d_i in two different ways: 1) affecting the amount of B-cells produced and 2) affecting the killing rate of virus by B-cells. Virus grows at a rate r and is eliminated by B-cells at a rate k. With these hypothesis, we obtain the following system of ordinary differential equations

$$\begin{aligned} \text{Virus:} \quad & \frac{dV}{dt} = rV - f(d_i)kVB_i \\ \text{For } i = 1, \ldots, n\text{:} & \\ \text{B-cells:} \quad & \frac{dB_i}{dt} = \sigma B_i * \frac{V}{\frac{\phi}{f(d_i)} + V} \end{aligned} \tag{1}$$

Model 2: We next add uninfected cells U, infected cells I, and antibodies to our model, obtaining a target-cell limitation model, similar to the classic viral kinetic model ([10, 11]). In this model, uninfected cells U become infected I upon contact with virus V with infectivity β. We assume no target-cell production or death given the short timespan of an influenza infection, but infected cells have an increased death rate. In addition, for each clone, B-cells are stimulated and produce antibodies which in turn clear virus. For each clone, B-cell stimulation, antibody production and the antibody's ability to remove virus are modulated by a function that depends on the antigenic distance between that clone and the virus. Table S1 describes the parameters used for this model and presented in the results. The corresponding ordinary differential equations are given by

$$\begin{aligned} \text{Uninfected cells:} \quad & \frac{dU}{dt} = -\beta UV \\ \text{Infected cells:} \quad & \frac{dI}{dt} = \beta UV - \delta_I I \\ \text{Virus:} \quad & \frac{dV}{dt} = p_I I - \delta_V V - kV \sum_{i=1}^{n} f(d_i) A_i \\ \text{For } i = 1, \ldots, n\text{:} & \\ \text{B-cells:} \quad & \frac{dB_i}{dt} = \sigma B_i * \frac{V}{\frac{\phi}{f(d_i)} + V} \\ \text{Antibodies:} \quad & \frac{dA_i}{dt} = p_B B_i - \delta_A A_i \end{aligned} \tag{2}$$

Model 3: This model builds upon the last one by adding innate immunity. Innate immunity in this model causes uninfected cells to become refractory to infection. This is modeled by the removal of cells from the U population at a rate proportional to the amount of innate immunity (which is in turn proportional to the number of infected cells).

$$\begin{aligned} \text{Uninfected cells:} \quad & \frac{dU}{dt} = -\beta UV - k_X UI \\ \text{Infected cells:} \quad & \frac{dI}{dt} = \beta UV - \delta_I I \\ \text{Virus:} \quad & \frac{dV}{dt} = p_I I - \delta_V V - kV \sum_{i=1}^{n} f(d_i) A_i \\ \text{For } i = 1, \ldots, n\text{:} & \\ \text{B-cells:} \quad & \frac{dB_i}{dt} = \sigma B_i * \frac{V}{\frac{\phi}{f(d_i)} + V} \\ \text{Antibodies:} \quad & \frac{dA_i}{dt} = p_B B_i - \delta_A A_i \end{aligned} \tag{3}$$

Model 4: In this model we add an equation to explicitly model innate immunity X. Innate immunity grows in a logistic fashion at rate σ_X, and it is modulated by the amount of virus present in the system via a saturation function, where ϕ_X represents the half-saturation constant. Finally, innate immunity decays at a rate δ_X,

$$\begin{aligned}
\text{Uninfected cells:} \quad & \frac{dU}{dt} = -\beta UV - k_X UX \\
\text{Infected cells:} \quad & \frac{dI}{dt} = \beta UV - \delta_I I \\
\text{Virus:} \quad & \frac{dV}{dt} = p_I I - \delta_V V - kV \sum_{i=1}^{n} f(d_i) A_i \\
\text{Innate-immunity} \quad & \frac{dX}{dt} = \sigma_X (100 - X) \frac{V}{\phi_X + V} - \delta_X X \\
\text{For } i = 1, \ldots, n\text{:} & \\
\text{B-cells:} \quad & \frac{dB_i}{dt} = \sigma B_i * \frac{V}{\frac{\phi}{f(d_i)} + V} \\
\text{Antibodies:} \quad & \frac{dA_i}{dt} = p_B B_i - \delta_A A_i
\end{aligned} \tag{4}$$

For each of these models, we simulate a primary infection followed by vaccination and then an epidemic challenge as follows:

- **Pre-existing immunity simulation:** We run the model for a virus closest to clone 1 (arbitrary) to obtain pre-existing concentrations of B-cell and antibody clones.
- **Vaccination simulation:** We run the model for an attenuated virus. We consider two ways in which a vaccine strain can be attenuated: either by reducing its growth rate or infectivity ($\beta_{vac} < \beta$) and/or by increasing the rate at which antibodies remove virus ($k_{vac} > k$). We obtain new concentrations of B-cell and antibody clones. We assume that a vaccine "takes" (a vaccine mounts an appropriate immune response) if it generates a viral load comparable to that of a non-attenuated virus, which results in turn in the stimulation of B-cell clones and hence production of antibodies closest to the virus.
- **Epidemic Challenge simulation:** We then simulate an epidemic challenge by running the equations for a third, different virus, utilizing the B-cell and antibody concentrations obtained after vaccination. We varied the antigenic distance from challenge strain to pre-existing immunity.

For all of these models, Clones closer to the virus will have a rapid expansion while those antigenically different will not be stimulated. B-cells do not grow indefinitely, indeed, the B-cell equations in all our models have saturation terms. We use the area under the curve (AUC) as a measure of immune control, if $AUC < 2$ (logarithmic scale) the infection was controlled. We then varied (while keeping pre-existing immunity always centered around clone 1) the distances between vaccine and pre-existing immunity, vaccine and challenge, and challenge and pre-existing immunity (denoted by $d(V, PI)$, $d(V, C)$ and $d(C, PI)$ respectively) to study how the interplay of these antigenic distances affected the ability of the vaccine to *i)* mount an appropriate immune response (that is, the ability of the vaccine to "take", regardless of what the epidemic challenge would be) and *ii)* the ability of the vaccine to control subsequent infections with an epidemic challenge. In the main text, we defined the within-host vaccine effect, ve_ω, that quantifies the extent to which a vaccine was able to prevent further infections. With a low ve_ω, a vaccinated individual will see little additional benefit compared to that same individual had s/he not been vaccinated when presented with subsequent challenge infections with that particular strain. In contrast, a high ve_ω implies that the vaccine was the responsible for controlling subsequent infections with that challenge strain. The within-host effect is a function of both the vaccine strain and the challenge strain.

Sensitivity analysis

We performed sensitivity analysis by varying our models and our parameters. Our results were consistent over a variety of parameter values for all the models considered. The different assumptions leading to our different models

did not qualitatively alter our results, but, as expected, they altered the shape and particular range of values for which the conclusions hold. We varied the cross reactivity of antibodies by varying the antibody affinity to virus so that they stop being reactive to virus once their antigenic distance to virus was 15% to 40% (figs. S5, S6, S7, S8). When the antibodies are less cross-reactive, then as expected, vaccine and pre-existingn immunity stop being protective when their distance to the challenge is smaller ($d(V, PI) \sim 10\%$). Under this scenario, there is a wider range of values for which choosing a vaccine strain farther away from pre-existing immunity would result in a better control of subsequent challenges (Fig. S5). The area for which the within-host vaccine effect is high follows the diagonal (so the vaccine will be highly efficacious for vaccines matched to the epidemic strain if both are sufficiently different from pre-existing immunity), see Fig. S7. When the antibodies are more cross reactive, our models predict that pre-existing immunity will control the epidemic challenge and the vaccine strain for a wider range of antigenic distances, resulting in a smaller range where the vaccine will be immunogenic (Fig. S6 and Fig. S8).

In addition, we varied the number of clones in our model. As seen in figures S9 - S15, our results are not sensitive to this parameter. The contour plots for all the models considered exhibit a similar qualitative behaviour, regardless of the number of clones. However, for low number of clones ($n = 10$), the region of the contour plot resulting in a low severity of infection is slightly bigger (for challenge strains for which the distance to pre-existing immunity is big) than that observed for 15 or more clones.

Supplemental Figures

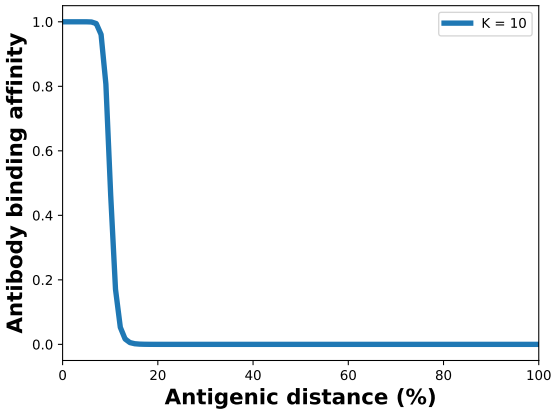

Figure S1: Antibody binding efficacy as a function of antigenic distance. The antigenic distance given in [1] was used for the simulations. This antigenic distance is defined as the number of point mutations needed to go from one antigen (or antibody) to another antigen (or antibody). Full details above.

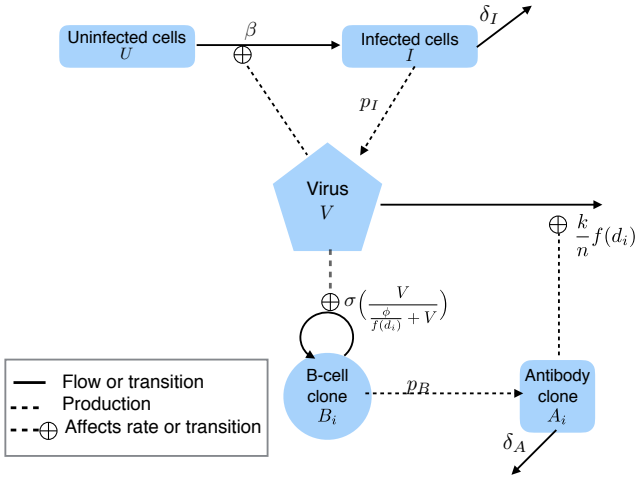

Figure S2: Diagram of Model 2. Uninfected cells U become infected I upon contact with virus V. Infected cells produce virus at rate p_I and are removed at rate δ_I. B-cells are produced at a rate σ, They are further divided into n distinct clones and produce antibodies at rate p_B. Antibodies are removed at rate δ_A and eliminate virus at a rate proportional to their antigenic distance to the virus (d_i with $i = 1, \ldots, n$), determined by the function $f(d_i)$.

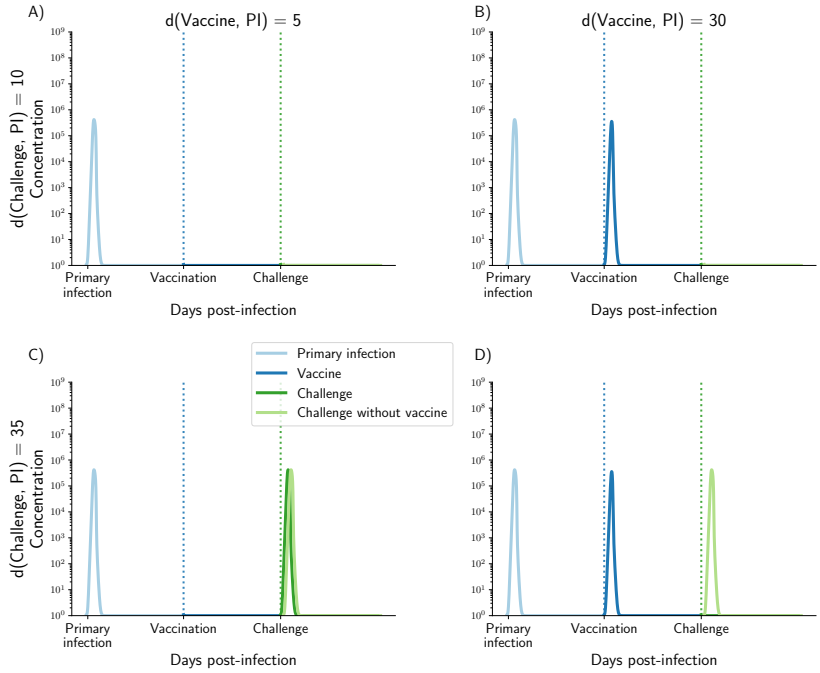

Figure S3: Viral load curves for 4 different scenarios depending on the antigenic distance between pre-existing immunity, vaccine strain and challenge strain. Top row (A and B): challenge strain is 10% different from pre-existing immunity, bottom row (C and D): challenge strain is 35% different from pre-existing immunity. Left panels (A and C) vaccine strain is 5% different from pre-existing immunity, right panels (B and D): vaccine is 30% different. Distance between vaccine and challenge: 5%, 20%, 30% and 5% respectively for panels A-D

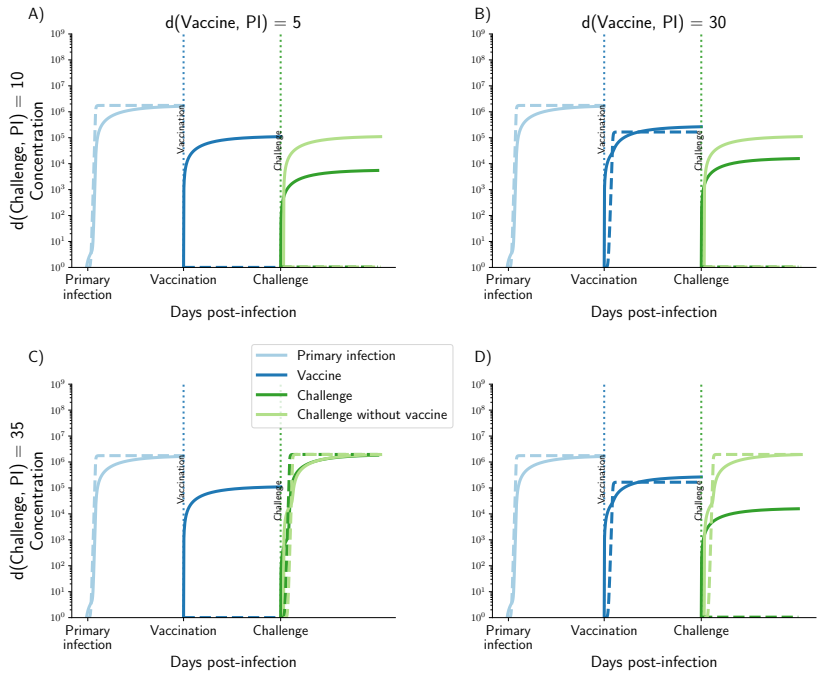

Figure S4: Total B-cell (dashed lines) and antibody (solid lines) dynamics for 4 different scenarios depending on the antigenic distance between pre-existing immunity, vaccine strain and challenge strain. Top row (A and B): challenge strain is 10% different from pre-existing immunity, bottom row (C and D): challenge strain is 35% different from pre-existing immunity. Left panels (A and C) vaccine strain is 5% different from pre-existing immunity, right panels (B and D): vaccine is 30% different. Distance between vaccine and challenge: 5%, 20%, 30% and 5% respectively for panels A-D

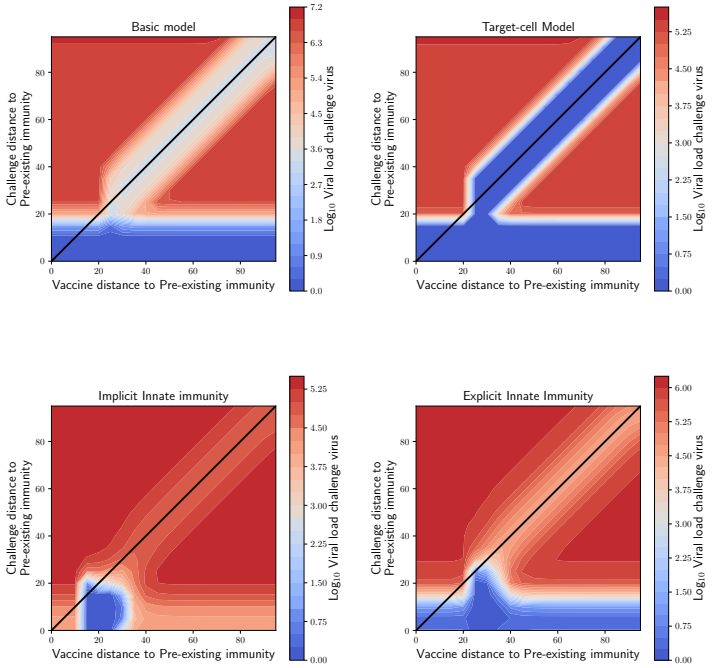

Figure S5: Sensitivity analysis for the contour plots representing the severity of infection presented in the main text when the antibodies are less cross-reactive. Here, the parameters for the Hill function were $K = 8$, $p = 10$. This results in antibodies that stop being reactive to a virus once their antigenic distance differs by $\sim$15%.

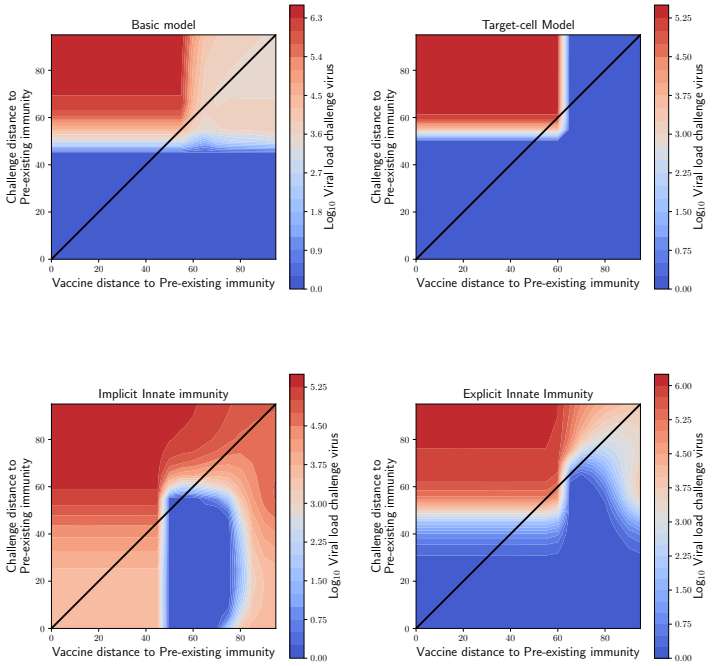

Figure S6: Sensitivity analysis for the contour plots representing the severity of infection presented in the main text when the antibodies are more cross-reactive. Here, the parameters for the Hill function were $K = 25$, $p = 15$. This results in antibodies that stop being reactive to a virus once their antigenic distance differs by $\sim$40%.

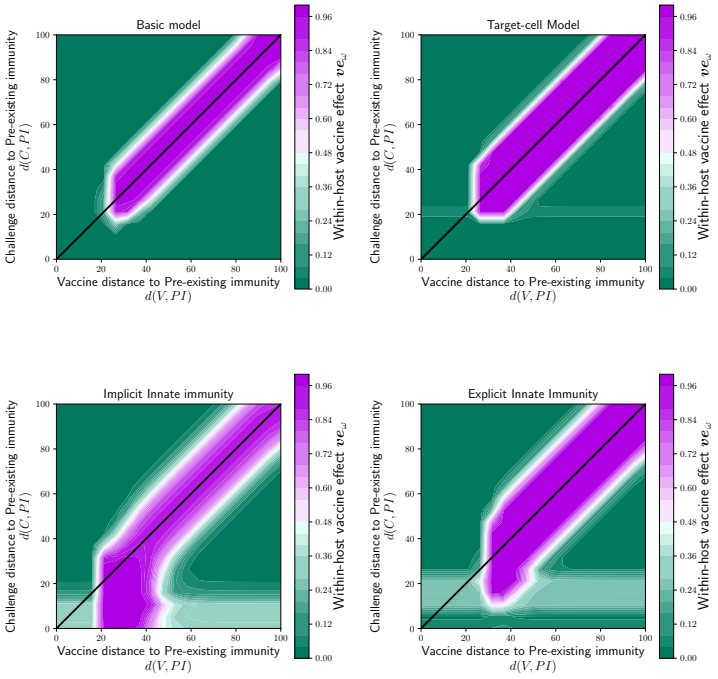

Figure S7: Sensitivity analysis for the within-host vaccine effect contour plots presented in the main text when the antibodies are less cross-reactive. Here, the parameters for the Hill function were $K = 8$, $p = 10$. This results in antibodies that stop being reactive to a virus once their antigenic distance differs by $\sim$15%.

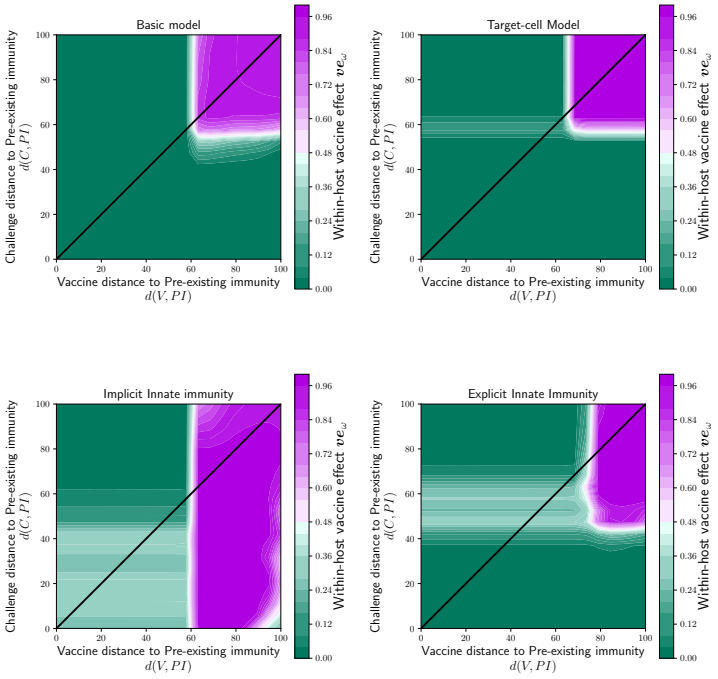

Figure S8: Sensitivity analysis for the within-host vaccine effect contour plots presented in the main text when the antibodies are more cross-reactive. Here, the parameters for the Hill function were $K = 25$, $p = 15$. This results in antibodies that stop being reactive to a virus once their antigenic distance differs by $\sim$40%.

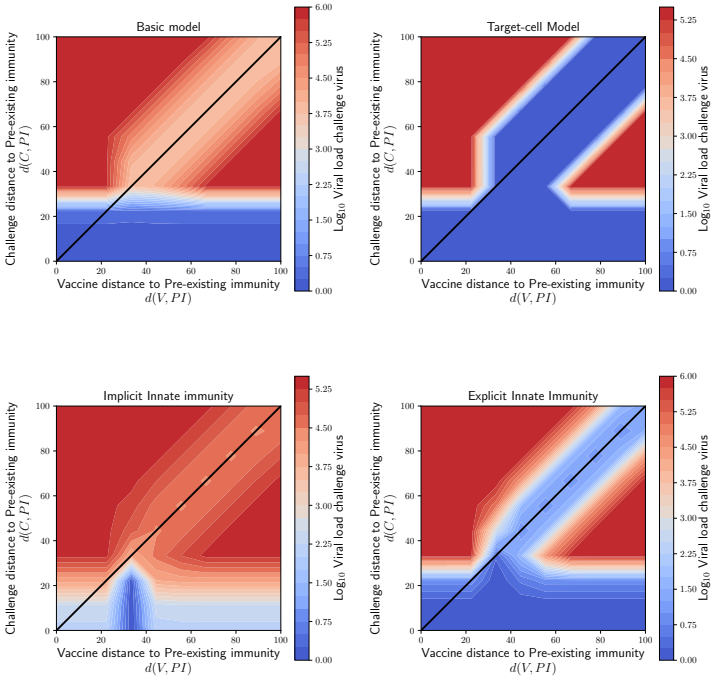

Figure S9: Sensitivity analysis for the contour plots representing the extent of viral replication for a challenge infection with 10 B-cell clones. These results are qualitatively similar to those presented in the main text, but the area resulting in a contained infection is slightly bigger with fewer number of clones.

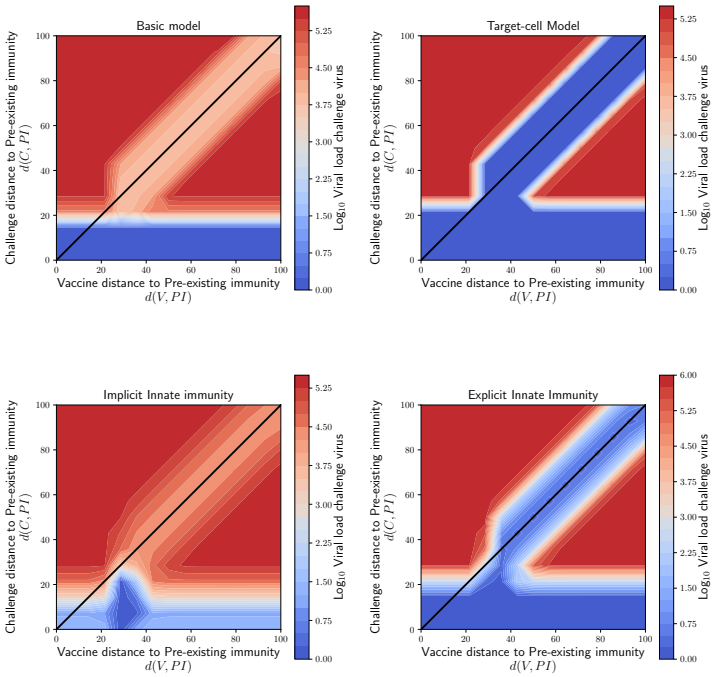

Figure S10: Sensitivity analysis for the contour plots representing the extent of viral replication for a challenge infection with 15 B-cell clones. These results are qualitatively similar to those presented in the main text.

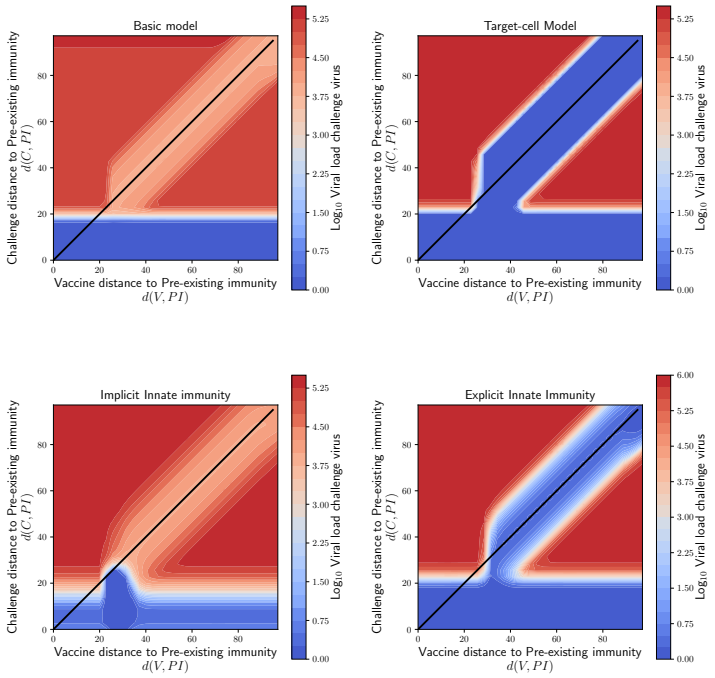

Figure S11: Sensitivity analysis for the contour plots representing the extent of viral replication for a challenge infection with 35 B-cell clones. These results are qualitatively similar to those presented in the main text.

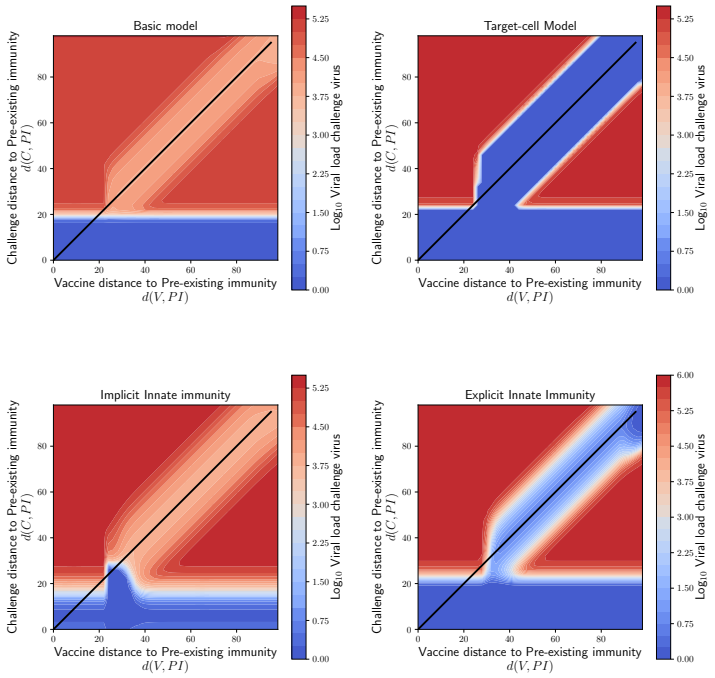

Figure S12: Sensitivity analysis for the contour plots representing the extent of viral replication for a challenge infection with 50 B-cell clones. These results are qualitatively similar to those presented in the main text

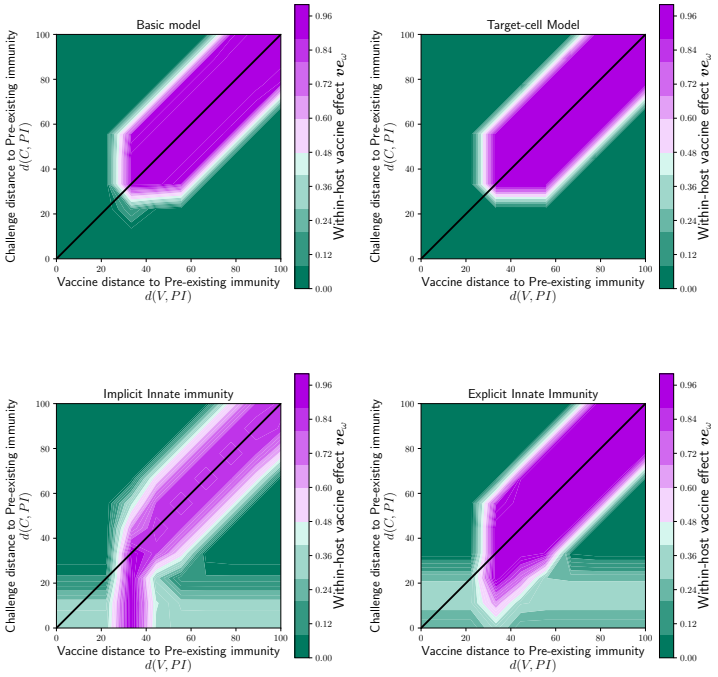

Figure S13: Sensitivity analysis for the contour plots representing the within-host vaccine effect with 10 B-cell clones.

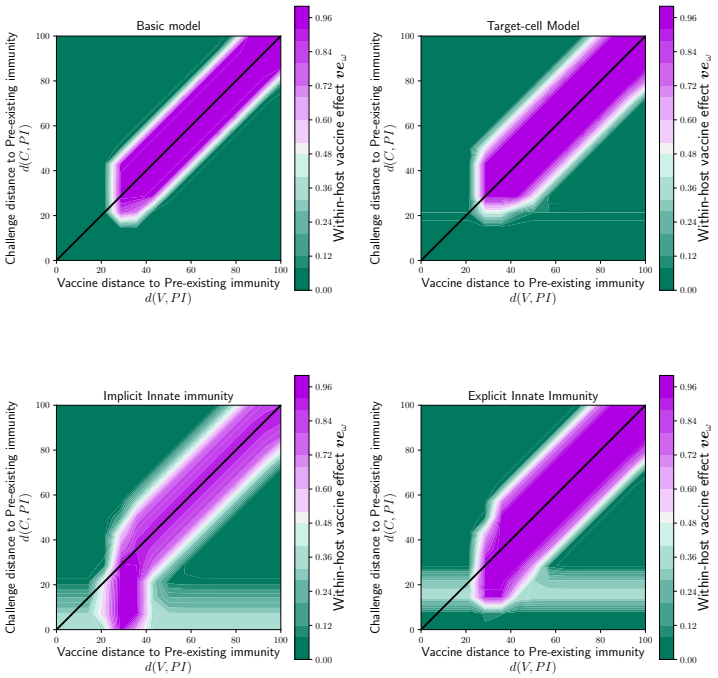

Figure S14: Sensitivity analysis for the contour plots representing the within-host vaccine effect with 15 B-cell clones.

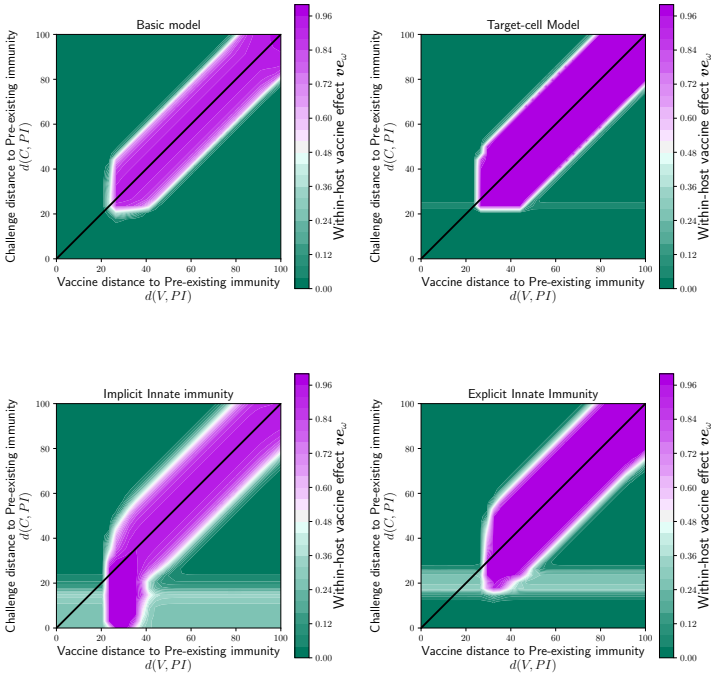

Figure S15: Sensitivity analysis for the contour plots representing the within-host vaccine effect with 35 B-cell clones.

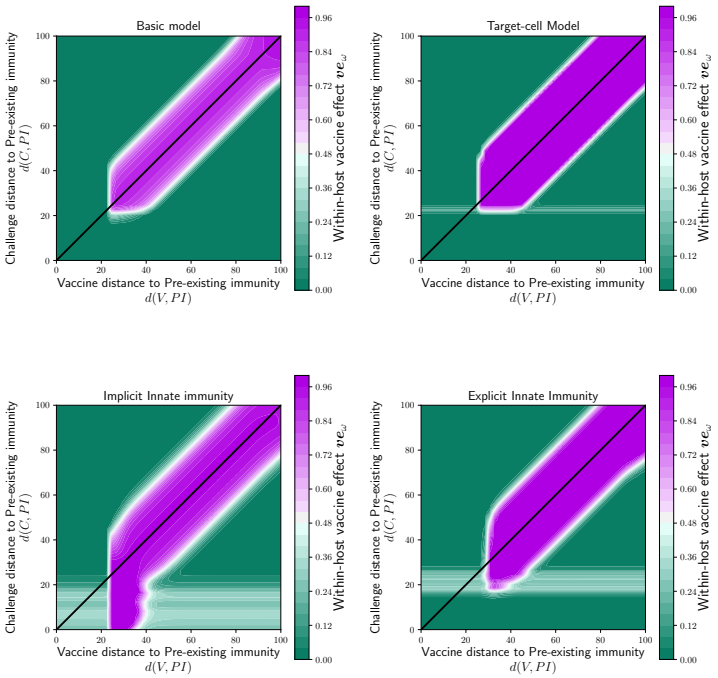

Figure S16: Sensitivity analysis for the contour plots representing the within-host vaccine effect with 50 B-cell clones.

Tables

Table S1: Model 2 used in the main text: parameters definitions and values.

Model parameter	Symbol	Units	Value	Reference
Virus infection rate	β		$2.7 * 10^{-5}$	[6]
Virus infection rate for vaccine strain	β_{Vac}		$(0.1 - 1) * \beta$	varied
Death rate for infected cells	δ_I	day^{-1}	4.0	[6]
Virus production rate	p_I	day^{-1}	$1.2 * 10^{-2}$	[6]
Antibody death rate	δ_A	day^{-1}	10^{-1}	[12]
Virus clearance rate	δ_V	day^{-1}	3	[6]
Infected cell killing rate by antibodies	k	day^{-1}	$5 * 10^{-3}$	scaled
Infected cell killing rate by antibodies for vaccine virus	k_{Vac}	day^{-1}	$(10 - 50) * k$	varied
Number of virus for half-max. B-cell activation	ϕ		$5 * 10^3$	scaled [a]
Max. activation rate of B-cells	σ_B		10	scaled
Rate of production of antibodies by B-cells	p_B	day^{-1}	10^{-1}	scaled

[a] These parameters were scaled so that the B-cells and antibodies were at equilibrium when no infection is present.

Table S2: Parameters for all models

Model parameter	Symbol	**Model1**	**Model2**	**Model3**	**Model4**
Virus growth rate	r	1.0	–	–	–
Virus infection rate	β	–	$2.7 * 10^{-5}$	$2.7 * 10^{-5}$	$2.7 * 10^{-5}$
Virus infection rate for vaccine strain	β_{Vac}		$(0.1 - 1) * \beta$		
Saturation constant for B-cell production	c	–	–	–	–
Death rate for infected cells	δ_I	–	4	4	4
Virus production rate	p_I	–	$7.1 * 10^{-2}$	$7.1 * 10^{-2}$	$7.1 * 10^{-2}$
Antibody death rate	δ_A	–	10^{-1}	10^{-1}	10^{-1}
Virus clearance rate	δ_V	–	3.0	3.0	3.0
Innate immunity death rate	δ_X	–	–	–	0.2
Infected cell killing rate by antibodies	k	–	$5 * 10^{-3}$	$5 * 10^{-3}$	$5 * 10^{-3}$
Infected cell killing rate by antibodies for vaccine virus	k_{Vac}	–	$(1 - 50) * k$	$(1 - 50) * k$	$(1 - 50) * k$
Infected cell killing rate by innate immunity	k_X	–	–	10^{-6}	10^{-1}
Number of virus for half-max. B-cell activation	ϕ_B	10^3	$5 * 10^3$	1.0	10
Number of infected cells for half-max. innate immunity activation	ϕ_X	–	–	–	1
Max. activation rate of B-cells	σ_B	1.0	10	2.0	2.0
Max. activation rate of innate immunity	σ_X	–	–	–	$5 * 10^{-1}$
Rate of production of antibodies by B-cells	p_B	–	10^{-1}	10^{-1}	10^{-1}

References

[1] D J Smith, S Forrest, D H Ackley, and A S Perelson. Variable efficacy of repeated annual influenza vaccination. *Proc Natl Acad Sci U S A*, 96(24):14001–14006, Nov 1999. ISSN 0027-8424 (Print); 0027-8424 (Linking).

[2] Danuta M Skowronski, Catharine Chambers, Gaston De Serres, Suzana Sabaiduc, Anne-Luise Winter, James A Dickinson, Jonathan B Gubbay, Kevin Fonseca, Steven J Drews, Hugues Charest, Christine Martineau, Mel Krajden, Martin Petric, Nathalie Bastien, Yan Li, and Derek J Smith. Serial Vaccination and the Antigenic Distance Hypothesis: Effects on Influenza Vaccine Effectiveness During A(H3N2) Epidemics in Canada, 2010-2011 to 2014-2015. *J Infect Dis*, 215(7):1059–1099, Apr 2017. ISSN 1537-6613 (Electronic); 0022-1899 (Linking). doi: 10.1093/infdis/jix074.

[3] Zhipeng Cai, Tong Zhang, and Xiu-Feng Wan. Antigenic distance measurements for seasonal influenza vaccine selection. *Vaccine*, 30(2):448–453, Jan 2012. ISSN 1873-2518 (Electronic); 0264-410X (Linking). doi: 10.1016/j.vaccine.2011.10.051.

[4] Derek J Smith, Alan S Lapedes, Jan C de Jong, Theo M Bestebroer, Guus F Rimmelzwaan, Albert D M E Osterhaus, and Ron A M Fouchier. Mapping the antigenic and genetic evolution of influenza virus. *Science*, 305 (5682):371–376, Jul 2004. ISSN 1095-9203 (Electronic); 0036-8075 (Linking). doi: 10.1126/science.1097211.

[5] Michael W Deem and Keyao Pan. The epitope regions of H1-subtype influenza A, with application to vaccine efficacy. *Protein Eng Des Sel*, 22(9):543–546, Sep 2009. ISSN 1741-0134 (Electronic); 1741-0126 (Linking). doi: 10.1093/protein/gzp027.

[6] Prasith Baccam, Catherine Beauchemin, Catherine A Macken, Frederick G Hayden, and Alan S Perelson. Kinetics of influenza A virus infection in humans. *J Virol*, 80(15):7590–7599, Aug 2006. ISSN 0022-538X (Print); 0022-538X (Linking). doi: 10.1128/JVI.01623-05.

[7] Kasia A Pawelek, Giao T Huynh, Michelle Quinlivan, Ann Cullinane, Libin Rong, and Alan S Perelson. Modeling within-host dynamics of influenza virus infection including immune responses. *PLoS Comput Biol*, 8(6): e1002588, 2012. doi: 10.1371/journal.pcbi.1002588.

[8] Roberto A Saenz, Michelle Quinlivan, Debra Elton, Shona Macrae, Anthony S Blunden, Jennifer A Mumford, Janet M Daly, Paul Digard, Ann Cullinane, Bryan T Grenfell, John W McCauley, James L N Wood, and Julia R Gog. Dynamics of influenza virus infection and pathology. *J Virol*, 84(8):3974–83, Apr 2010. doi: 10.1128/JVI.02078-09.

[9] Catherine A A Beauchemin and Andreas Handel. A review of mathematical models of influenza A infections within a host or cell culture: lessons learned and challenges ahead. *BMC Public Health*, 11 Suppl 1:S7, 2011. doi: 10.1186/1471-2458-11-S1-S7.

[10] A S Perelson, D E Kirschner, and R De Boer. Dynamics of HIV infection of CD4+ T cells. *Math Biosci*, 114(1): 81–125, Mar 1993. ISSN 0025-5564 (Print); 0025-5564 (Linking).

[11] M A Nowak, A L Lloyd, G M Vasquez, T A Wiltrout, L M Wahl, N Bischofberger, J Williams, A Kinter, A S Fauci, V M Hirsch, and J D Lifson. Viral dynamics of primary viremia and antiretroviral therapy in simian immunodeficiency virus infection. *J Virol*, 71(10):7518–7525, Oct 1997. ISSN 0022-538X (Print); 0022-538X (Linking).

[12] M K Slifka, R Antia, J K Whitmire, and R Ahmed. Humoral immunity due to long-lived plasma cells. *Immunity*, 8(3):363–372, Mar 1998. ISSN 1074-7613 (Print); 1074-7613 (Linking).